International Journal of Pharmaceutics 467 (2014) 60–69

Contents lists available at ScienceDirect

International Journal of Pharmaceutics

journal homepage: www.elsevier.com/locate/ijpharm

Silicon microfluidic flow focusing devices for the production of size-controlled PLGA based drug loaded microparticles

Kieran Keohane [a], Des Brennan [b], Paul Galvin [b], Brendan T. Griffin [a,*]

[a] Pharmacodelivery Group, School of Pharmacy, University College Cork, Ireland
[b] Tyndall National Institute, University College Cork, Ireland

ARTICLE INFO

Article history:
Received 5 February 2014
Received in revised form 24 March 2014
Accepted 26 March 2014
Available online 28 March 2014

Keywords:
Microfluidics
Ciclosporin A
PLGA
PEG-PLGA
Monodisperse
Controlled release

ABSTRACT

The increasing realisation of the impact of size and surface properties on the bio-distribution of drug loaded colloidal particles has driven the application of micro fabrication technologies for the precise engineering of drug loaded microparticles. This paper demonstrates an alternative approach for producing size controlled drug loaded PLGA based microparticles using silicon Microfluidic Flow Focusing Devices (MFFDs). Based on the precise geometry and dimensions of the flow focusing channel, microparticle size was successfully optimised by modifying the polymer type, disperse phase (Q_d) flow rate, and continuous phase (Q_c) flow rate. The microparticles produced ranged in sizes from 5 to 50 μm and were highly monodisperse (coefficient of variation <5%). A comparison of Ciclosporin (CsA) loaded PLGA microparticles produced by MFFDs vs conventional production techniques was also performed. MFFDs produced microparticles with a narrower size distribution profile, relative to the conventional approaches. *In-vitro* release kinetics of CsA was found to be influenced by the production technique, with the MFFD approach demonstrating the slowest rate of release over 7 days (4.99 ± 0.26%). Finally, MFFDs were utilised to produce pegylated microparticles using the block co-polymer, PEG-PLGA. In contrast to the smooth microparticles produced using PLGA, PEG-PLGA microparticles displayed a highly porous surface morphology and rapid CsA release, with 85 ± 6.68% CsA released after 24 h. The findings from this study demonstrate the utility of silicon MFFDs for the precise control of size and surface morphology of PLGA based microparticles with potential drug delivery applications.

1. Introduction

Biodegradable microparticles have widespread applications in the drug delivery domain, including protein/peptide, vaccine and gene delivery strategies. The processing techniques for producing drug loaded microparticles require precise control of size and surface morphology of the microparticles formed, using rapid and scalable preparation steps with minimal loss of drug. Increasingly, the size and shape of drug loaded microparticles is considered a key determinant of *in-vivo* bio-distribution and efficacy (Petros and Desimone, 2010). Micro-engineering strategies are therefore required in the production of size-controlled and surface functionalised drug loaded microparticles.

Microfluidic Flow Focusing Devices (MFFDs) are a *lab-on-chip* platform designed to manipulate fluid flow in microchannels with high precision and reduced consumption of reagents (Hung and Lee, 2007). This microfabrication technology is an evolving field for a diverse range of applications (Bashir, 2004). Its applications in point-of-care testing (POCT), high throughput screening, and bioanalysis have previously been reported (Whitesides, 2006; Yager et al., 2006). The potential for microfluidics as a platform in the fabrication of drug delivery systems has recently been recognised (Zhang et al., 2013; Gañán-Calvo et al., 2013).

Many of the conventional techniques utilised to produce biodegradable PLGA based microparticles, such as spray drying and emulsification/solvent evaporation (ESE), incorporate a "top-down" fabrication approach involving microparticle production following breakup of a larger bulk emulsion phase. Control of microparticle size with such "top-down" approaches is dependent on externally controlled parameters, such as homogenisation, sonication or jet break-up of the bulk emulsion. This can necessitate extended processing phases to achieve appropriate microparticle size and reduce polydispersity, which may also have

* Corresponding author at: School of Pharmacy, Cavanagh Pharmacy Building, University College Cork, College Road, Cork, Ireland. Tel.: +353 21 4901657.
E-mail address: brendan.griffin@ucc.ie (B.T. Griffin).

http://dx.doi.org/10.1016/j.ijpharm.2014.03.051
0378-5173/

detrimental effects on drug loadings and encapsulation efficiencies (Paudel et al., 2013). Particle morphology also tends to be poorly controlled and highly dependent on experimental procedures, such as polymer concentration, agitation conditions, and the rate of solvent elimination (Rosca et al., 2004).

Recently, other key enabling microfabrication technologies have been investigated to produce PLGA based microparticles. Low Temperature Co-fired Ceramic (LTCC) micromixers utilise a modified process based upon the traditional emulsification/solvent evaporation technique to produce drug loaded microspheres (Ribeiro-Costa et al., 2009). A similar microfabrication technique is microfluidisation. Unlike LTCC micromixers, microfluidisation utilises a high pressure chamber to facilitate liquid movement in the microchannels to the point where droplet impingement occurs to produce smaller droplet sizes. However, the difficulties with instrument operation, cleaning, and scale-up make microfluidisation less favourable than conventional processing techniques (Maa and Hsu, 1999).

Microfluidics involves hydrodynamic manipulation of fluids in microchannels with dimensions of tens of micrometres. Droplet-based microfluidics is a subcategory of microfluidics that, in contrast with continuous (or analogical) microfluidics, can independently control discrete volumes of fluids in immiscible phases with low Reynolds number and laminar flow regimes, enabling precise control of microparticle formation (Gañán-Calvo et al., 2013). MFFDs therefore offer an alternative "bottom-up" approach to microparticle production and the potential to address some of the limitations associated with conventional processing techniques (Kang et al., 2008). MFFDs incorporate flows of two immiscible fluids in microchannels: the continuous phase and the disperse phase (containing drug and polymer). The continuous phase (Q_c) is injected through two outside channels and the disperse phase (Q_d) is injected through a central channel into a flow focusing junction (Fig. 1). Fluid dynamics at the flow focusing region governs droplet break up, where droplets of the disperse phase are produced as a result of the shear force and interfacial tension at the fluid–fluid interface (Whitesides, 2006).

Microfluidics has previously demonstrated utility in the production of hydrogel based microparticles using the water soluble polymers, alginate and methacrylate (Yeh et al., 2009; De Geest et al., 2005). Poly(D,L lactide-co-glycolide) (PLGA) polymer has been chosen in this study as it is biocompatible, GRAS approved, and is widely utilised for the sustained release of both polar and non-polar drugs. The potential of microfluidics to produce PLGA microparticles has previously been reported utilising a polydimethylsiloxane (PDMS)-based MFFD device (Xu et al., 2009). However, poor compatibility of PDMS with organic solvents is a significant limitation, resulting in wetting and swelling of the microchannel walls, which oftentimes necessitates a surface pre-treatment step. The current study advances the aforementioned by utilising a more robust silicon MFFD device that is resistant to organic solvents (e.g. dichloromethane), does not require a surface pre-treatment step, is capable of withstanding high fluid flow rates and is amenable to scale-up applications.

The aim of this work was to investigate the potential of silicon based MFFDs to produce precisely controlled drug loaded PLGA based microparticles. Ciclosporin A (CsA) was chosen as a model peptide for evaluation of drug release characteristics. Fluid dynamics at the flow-focusing junction were optimised to generate monodisperse microparticles in the outlet channel. A comparison of PLGA based microparticles produced by MFFDs vs conventional production techniques was performed. The potential to produce microparticles using PEG-PLGA block co-polymers was also evaluated.

2. Materials and methods

2.1. Materials

Ciclosporin A (CsA) (from *Tolypocladium inflatum*, purity ≥ 95%) was purchased from Sigma–Aldrich. Various types of Poly(D,L-lactide-co-glycolide) (Table 1) were purchased from Boehringer Ingelheim (Germany). HPLC grade dichloromethane, acetonitrile,

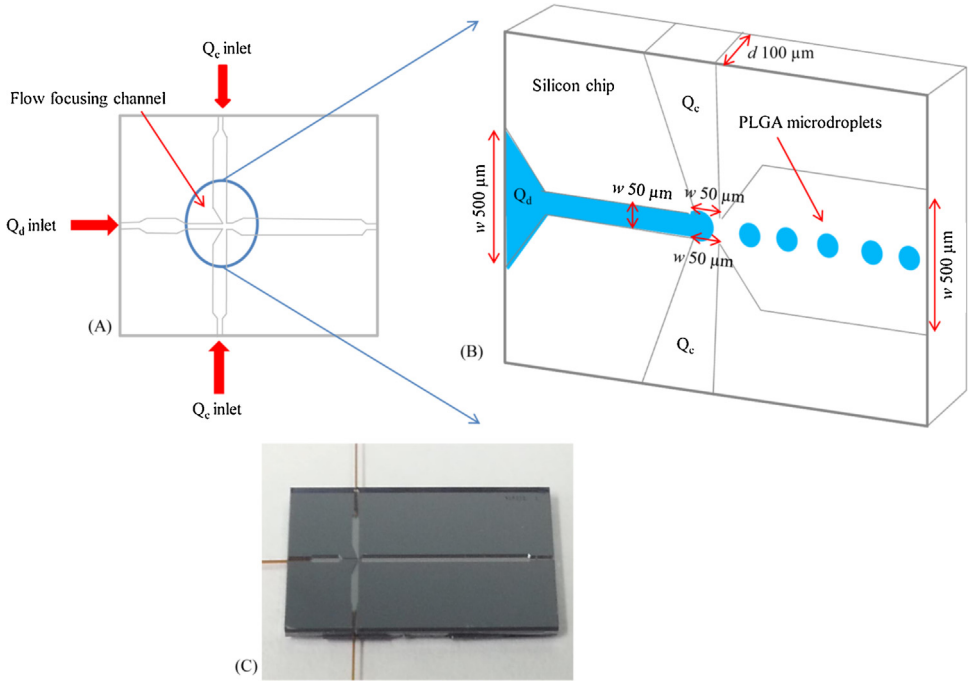

Fig. 1. (A) Schematic drawing of the silicon microfluidic chip. (B) Magnified view of the flow focusing region within the silicon microfluidic device. (C) Image of a fabricated silicon microfluidic device with glass capillary inserts (200 µm o.d.) in each inlet.

Table 1
Composition of the Resomer® PLGA polymers used.

Name	Polymer type	Composition	LA:GA ratio	PEG content (%)	Inherent viscosity (dl/g)
PLGA (Low viscosity)	Monoblock	PLGA	73:27	–	0.32
PLGA (Medium viscosity)	Monoblock	PLGA	85:15	–	0.55
PEG-PLGA	Diblock	PEG-PLGA 6000	1:1	10	0.72

and water were purchased from Sigma–Aldrich. All other chemicals and reagents were of analytical grade.

2.2. Fabrication of silicon microfluidic flow focusing devices

Silicon based MFFDs were fabricated using standard photolithographic and deep reactive ion etching (DRIE) processes (Lo et al., 2010). Access holes were patterned and etched onto the front side of a silicon wafer. The final device was sealed by anodic bonding of the silicon wafer to a heat resistant borosilicate glass wafer. The cross sectional dimensions of the flow focusing channel were 50 μm wide and 100 μm deep. The total length of the silicon microfluidic device was 25 mm. The silicon MFFDs were diced and a 1 mm access hole was drilled into the outlet channel using a Maxima® round bur drill bit (Henry Schein®). A Nanoport™ assembly (Upchurch Scientific®) containing a preformed adhesive ring was placed over the hole and heat sealed at 160 °C for 1 h. Fused glass capillaries (100 μm i.d., 200 μm o.d.) (Composite Metal Services, UK) were sealed to the inlet of the microchannels using UV optical adhesive (Norland products, Inc.). The capillaries connected the microchannels to the syringe pumps using polytetrafluoroethylene (PTFE) tubing sleeves and MicroTight® fittings (Upchurch Scientific).

2.3. Production of PLGA based microparticles using silicon MFFDs

The continuous phase (Q_c) consisted of an aqueous solution of PVA (1% w/v, M_w 6000, 80 mol% hydrolysed, Polysciences, Inc.) as surfactant. The disperse phase (Q_d) composed of 2.5 ml dichloromethane (DCM) containing 100 mg (4% w/v PLGA or PEG-PLGA copolymer and 20 mg (0.8% w/v) Ciclosporin A (CsA). The flow rates of Q_d and Q_c were optimised to facilitate droplet formation at the flow focusing channel and avoid co-laminar flows (Xu et al., 2009). The flow rates of Q_d ranged between 0.3 and 1.2 ml/h while the flow rates of Q_c were adjusted between 15 and 90 ml/h to facilitate uniform droplet formation at the flow focusing channel. Teflon tubing connected the Nanoport™ to a 250 ml round bottomed flask, which was suspended in approximately 10 ml of continuous phase (1% w/v PVA solution). At 30 min intervals, the round bottomed flask containing polymer microdroplets was removed and mounted on a rotary evaporator (Büchi, Switzerland). DCM solvent was removed under reduced pressure (100 mtorr) at 37 °C for 3 min. The hardened microparticles were collected in a 50 ml collection tube, centrifuged (4000 rpm, 3 min) and rinsed with deionised water three times to remove any residual surfactant. The supernatant was discarded and the microparticles were snap frozen in liquid nitrogen and lyophilised under reduced pressure (800 mtorr) at –80 °C for 24 h.

2.4. Production of PLGA microparticles using emulsification/solvent evaporation technique

Emulsification/solvent evaporation (ESE) was carried out based on a previous method with some minor modifications (Mao et al., 2008). A solution of 4% (w/v) PLGA or PEG-PLGA containing 100 mg CsA (0.8% w/v) was dissolved in 12.5 ml of DCM. This was added to 20 ml of 1% w/v aqueous PVA solution and homogenised using a paddle at 2000 rpm for 3 min (IKA®-WERKE, Germany). The resulting suspension was left stirring at room temperature for 4 h to evaporate the organic solvent. Residual solvent was removed under reduced pressure (70 mtorr) at 37 °C for 3 min using a rotary evaporator (Büchi, Switzerland). The suspension was then centrifuged at 4000 rpm for 3 min and washed three times with deionised water to remove residual surfactant. The supernatant was discarded and the microparticles were snap frozen in liquid nitrogen and lyophilised at –80 °C for 24 h at 800 mtorr.

2.5. Production of PLGA microparticles using the spray drying technique

Spray drying was carried out based on a similar method described previously with some modifications (Ramtoola et al., 2011). A solution containing 1000 mg of PLGA (4% w/v) and 200 mg CsA (0.8% w/v) was dissolved in 25 ml of dichloromethane (DCM) at room temperature and spray dried in a Büchi B290 mini spray dryer (Flawil, Switzerland) with a 0.5 mm spray nozzle diameter. The process parameters used were; feed rate 3 ml/min, aspirator setting (100%), inlet temperature (50 ± 2 °C), outlet temperature (37 ± 2 °C). The PLGA solution was spray dried using the closed loop system at a spray flow rate of 500 l/h and spray flow pressure of 6 bar. The spray dried product was recovered from the sample collector.

2.6. Microparticle characterisation

Microparticle size was carried out using a Malvern mastersizer to determine the volume mean diameter (VMD) and polydispersity of samples by laser light diffraction using the hydro 2000 SM small volume dispersion unit (Malvern Instruments). In brief, approximately 50 mg of drug loaded microparticles was weighed out and dispersed in 20 ml of 0.1% (w/v) tween 20 solution and sonicated for 10 min based on a method described previously (Mao et al., 2007). Volume mean diameter, D(v,0.5), was calculated at the midpoint of the entire size distribution. The Span was calculated as:

$$\text{Span} = \frac{D[v,0.9] - D[v,0.1]}{D[v,0.5]}$$

D[v, 0.9], D[v, 0.5], and D[v,0.1] are the particle size diameters determined at the 90th, 50th, and 10th percentile of particles sized, respectively (Buske et al., 2012).

2.7. Determination of Capillary number

The dimensionless *Capillary* (*Ca*) number was calculated using the following equation (Fu et al., 2012);

$$\text{Ca} = \frac{m v}{\gamma}$$

where μ is the viscosity of the continuous phase (mN s/m^2), v is the velocity of the continuous phase (m/s), and γ is the interfacial

tension between the disperse phase and continuous phase (mN/m).

Viscosity of the continuous phase (1% w/v PVA) was measured at ambient temperatures with a vibroviscometer (SV-10, A&D Company Ltd., Japan). 35 ml of the fluid was poured into a measurement vessel. Two sensor plates were immersed in the fluid sample and viscosity was measured by detecting the electric current necessary to resonate the sensor plates. Velocity of the continuous phase ranged from 3.2 m/s to 4.8 m/s based on the flow rates previously established (Section 2.3). Interfacial tension at the liquid–liquid interface was measured using the Du Noüy ring method by addition of the disperse phase (1% w/v low viscosity PLGA) and continuous phase in equal volumes (10 ml) to a beaker. The force required to raise the ring was measured and related to the interfacial tension between the two liquids. All results were analysed in triplicate.

2.8. Scanning electron microscopy

The shape and surface morphology of the microparticles was characterised by scanning electron microscopy (JEOL 5200M). Samples were mounted onto double sided adhesive tape attached to an aluminium stub and sputter coated with a layer of gold (69 nm) (Polaron SC500). The samples were examined under accelerating voltage (2–5 kV) at a 9 mm working distance.

2.9. Specific surface area

The specific surface area of the microparticles was determined by gas adsorption based on a similar method described previously (Buske et al., 2012). Samples were prepared by degassing under vacuum (N_2) at room temperature for 24 h. Measurements were determined using a Gemini VI surface area analyser (Micromeritics®), with pure nitrogen as adsorbate at a temperature of 77 K. The data was interpreted based on the Brunauer, Emmett and Teller (BET) adsorption isotherm equation (Brunauer et al., 1938). Each batch was analysed in triplicate.

2.10. *In-Vitro* CsA release

In-vitro CsA release was performed using a USP type IV flow through apparatus based on a method described previously (Bhardwaj and Burgess, 2010). The apparatus was equipped with 22.6 mm diameter cells and the temperature of the water bath was maintained at 37 °C. The bottom of each cell was filled with 2.0 g of 1 mm sized glass beads to create a laminar flow profile. For release studies, 40 mg of encapsulated CsA/PLGA or CsA/PEG-PLGA containing approximately 6.7 mg of CsA was weighed out and added to each dissolution cell. Release experiments were carried out over 7 days using the closed loop system at a flow rate of 4 ml/min. The dissolution media consisted of 250 ml of 0.1 M hydrochloric acid (HCL) and 0.5% (w/v) SDS (USP 32 CsA monograph). Sink conditions were maintained throughout the experiment. pH was adjusted to 7.4 using 37% (v/v) HCL. In the case of PLGA, 1 ml samples were collected every 24 h and filtered through a 0.45 μm membrane filter. In the case of PEG-PLGA, 1 ml samples were taken at 1, 2, 3, 4, 6, 8, 12, and 24 h timepoints. All samples were replenished with fresh media. *In-vitro* release experiments were carried out in triplicate ($n = 3$). CsA was quantified using a validated HPLC–UV method using a Kinetex® C18 column (4.6 × 100 mm, Phenomenex) at 214 nm. The flow rate of the acetonitrile:water (50:50%, v/v) mobile phase was 1 ml/min with a sample injection volume of 20 μl. The column temperature was maintained at 60 °C.

2.11. Encapsulation efficiency

Encapsulation efficiency (%EE) of the microparticles was determined by dissolving 11 mg of microparticles in 1 ml of dichloromethane. The solution was filtered through a 0.45 μm filter and the filtrate was analysed at 214 nm by HPLC-UV. %EE was evaluated by the following equation (Khan et al., 2013);

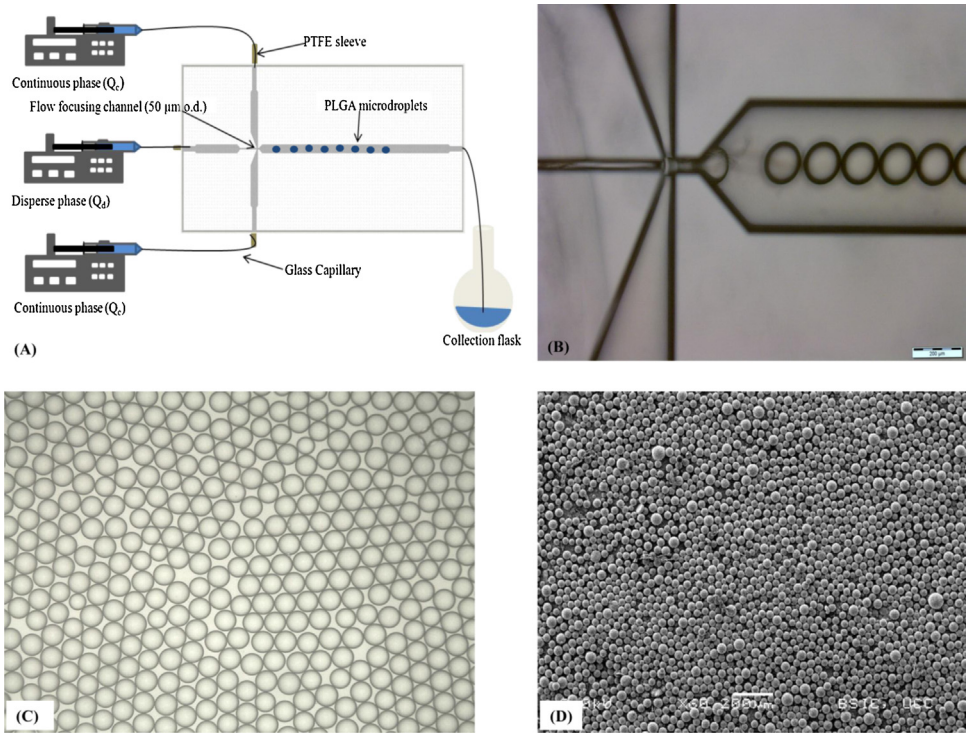

Fig. 2. (A) Illustration of the experimental setup procedure. (B) Image depicting droplet formation in the MFFD device. (C) and (D) Optical and scanning electron microscopy images of monodisperse PLGA (low viscosity) microparticles. Q_d:Q_c phase flow rate was 0.5:40 ml/h.

$$\%\text{Encapsulation efficiency} = \frac{\text{CsA encapsulated}}{\text{CsA total}} \times 100$$

2.12. Data analysis

Results are expressed as the mean ± standard deviation of three different samples. The difference between the means were assessed using one way analysis of variance (ANOVA) followed by a post-hoc Student's *T*-test. Results were considered statistically significant at $p < 0.05$.

3. Results

3.1. Generation of PLGA based microparticles on silicon MFFDs

Silicon based Microfluidic Flow Focusing Devices (MFFDs) were fabricated according to the protocol outlined in the methods section. The design incorporated a flow focusing geometry, where Q_c flowed perpendicular to Q_d. Initial studies were carried out to assess the potential to generate uniform droplet formation in the outlet channel of the MFFD device. Flow rates were optimised to yield uniform, monodisperse microdroplet formation, with an initial Q_d:Q_c flow rate of 0.5:40 ml/h, respectively. At high Q_c (40 ml/h), uniform droplet break up at the flow focusing channel was observed. The microparticles formed were collected, dried and visualised by electron microscopy. Highly uniform, spherical PLGA microparticles were observed (Fig. 2d). Particle size analysis confirmed the formation of a monodisperse size distribution, with mean $D_{(0.5)}$ particle size of 24.77 ± 0.96 μm and a coefficient of variation of 3.87%. Furthermore, the silicon based chips demonstrated significant improvements over comparable PDMS chips (in house data not shown), as silicon was solvent resistant, re-usable and capable of withstanding high fluid pressures.

3.2. Optimisation of processing conditions to generate size tuneable microparticles

The influence of formulation variables and fluid hydrodynamics on microparticle sizes was investigated. Firstly, the impact of disperse phase viscosity was evaluated utilising two different grades of PLGA [low viscosity (0.32 dl/g) and medium viscosity (0.55 dl/g)]. Both polymers were evaluated at 1%, 4%, and 8% (w/v) concentration at a fixed Q_d:Q_c flow rate of 0.5:40 ml/h (Fig. 3a). There was a significant decrease in microparticle size with low viscosity PLGA, in comparison to medium viscosity PLGA ($p < 0.05$). In addition, as polymer concentration increased, microparticle size decreased. Although this trend was observed with both PLGA grades, the size reduction was not significant at 4% and 8% (w/v) concentration with low viscosity PLGA.

The impact of fluid hydrodynamics on microparticle size was subsequently evaluated, by modifying Q_d and Q_c using 4% (w/v) PLGA (low viscosity) concentration (Fig. 3b). The Q_d flow rates selected were 0.3, 0.6, and 1.2 ml/h and the Q_c flow rates were 15, 30, and 60 ml/h. When Q_d was 0.3 ml/h, the smallest microparticle sizes were obtained when Q_c flow rate was highest i.e. 60 ml/h (7.62 ± 0.24 μm). This was smaller than the microparticle sizes obtained at Q_d:Q_c flow rates of 0.3:15 and 0.3:30 ml/h, respectively. Furthermore, at a constant Q_c flow rate, an increase in microparticle size was observed with increasing Q_d flow rate from 0.3 to 1.2 ml/h.

It has been previously reported that droplet formation is highly dependent on viscosity and interfacial forces. The relationship between *Ca* number and microparticle size was therefore evaluated using 1% (w/v) low viscosity PLGA solution (Fig. 3c). Results demonstrated that the smallest microparticles (5.29 ± 0.46 μm) were produced when *Ca* number was highest (0.212). At low *Ca* numbers (0.141), microparticle size increased

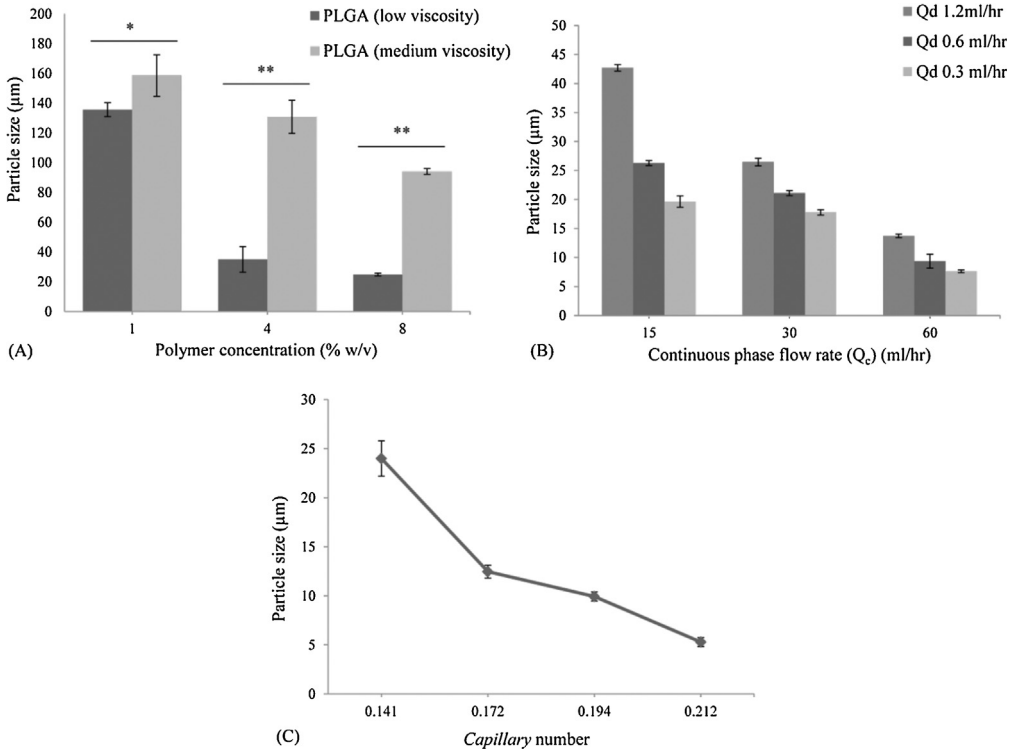

Fig. 3. (A) Effect of polymer viscosity on microparticle size at an initial Q_d:Q_c phase flow rate of 0.5:40 ml/h. (B) Influence of Q_d:Q_c phase flow rate on microparticle formation using PLGA (low viscosity) polymer. (C) Effect of *Capillary* number on microparticle size using 1% (w/v) PLGA (low viscosity) polymer. Q_d flow rate was 0.5 ml/h. Q_c flow rate was between 60 and 90 ml/h. Data represents the mean SD ($n = 3$). $^{*}p < 0.05$; $^{**}p < 0.01$ vs polymer viscosity.

approximately 5-fold (23.99 ± 1.81 μm). The calculated interfacial tension between Q_d and Q_c was 29 mN/m, while the viscosity of Q_c was 1.28 mPa.

3.3. Comparison of MFFDs with conventional production techniques

PLGA microparticles prepared using silicon MFFDs were compared to microparticles produced using both conventional techniques (spray drying, ESE), based on previous published procedures (Ramtoola et al., 2011; Sansdrap and Moës, 1993; Mao et al., 2008). The composition of the microparticles prepared using each processing technique is outlined in Table 2. As indicated in Fig. 4, the size of the PLGA microparticles produced by MFFDs was comparable in terms of $D_{(0.5)}$ to both spray drying and ESE. However, the span of the size distribution, defined as the width of microparticle size distribution at the 10th, 50th, and 90th percentile (Coimbra et al., 2008), was significantly smaller (1.53 ± 0.07) with MFFDs compared to the conventional processing techniques (5.39 ± 0.60, 6.08 ± 0.14, respectively) ($p < 0.01$). The morphology and surface aspect of the PLGA microparticles prepared using each technique was compared using SEM. The electron micrographs confirmed the highly uniform and monodisperse size of PLGA based microparticles obtained using silicon MFFDs (Fig. 5e and f), relative to both ESE and spray-drying (Fig. 5a–d).

In terms of drug loading, %EE of CsA loaded PLGA microparticles (95 ± 5%) was significantly higher than either spray drying or ESE ($p < 0.01$) (Table 3). The %EE of spray dried PLGA was only 54 ± 5%, which compared less favourably to ESE (69 ± 2%). Drug release characteristics of CsA from PLGA microparticles were evaluated in a type IV flow through apparatus. As indicated in Fig. 6, %CsA released from MFFD produced PLGA microparticles was lower compared to the both ESE and spray drying. Although no quantifiable CsA was detected for the first 2 days, from day 3 onwards, there was a gradual increase, which culminated in approximately 6% released after 7 days (5.99 ± 0.31%). By comparison, %CsA released from ESE and spray drying during the first 2 days were 4.94 ± 2.55% and 2.21 ± 0.40%, respectively. Cumulative release after 7 days was significantly higher at 20.51 ± 0.82% and 17.21 ± 1.12%, respectively ($p < 0.001$).

3.4. PEG-PLGA based microparticles produced using MFFDs

PEGylated PLGA based microparticles have attracted considerable interest as a means of providing a stearic surface barrier, minimising uptake by the reticuloendothelial system (RES) and prolonging the circulation half-life in blood (Karnik et al., 2008). The inclusion of a hydrophilic PEG moiety may also influence surface morphology and drug release characteristics (Ruan and Feng, 2003). Thus, the potential to produce PEG-PLGA microparticles was subsequently evaluated using MFFDs. The mean particle size of PEG-PLGA microparticles was 15.4 ± 0.1 μm (Table 3). This was approximately 2-fold larger compared to PLGA (i.e. non-pegylated) using similar flow rates (Q_d:Q_c 0.5:60 ml/h).

SEM images revealed the formation of porous, uniform PEG-PLGA microparticles using the MFFD technique (Fig. 7a and b). The highly porous 'sponge-like' structure was particularly noteworthy and in contrast to the polydisperse, irregular shaped PEG-PLGA microparticles produced using the ESE technique (Fig. 7c and d). The difference in surface morphology most likely reflected the controlled 'bottom-up' droplet formation with MFFDs vs the 'top-down' high shear generated droplet formation associated with ESE. Furthermore, as outlined in Table 3, MFFD produced PEG-PLGA batches had a significantly higher specific surface area (7.32 ± 0.02 m^2/g) compared to the same polymer produced using ESE (1.26 ± 0.01 m^2/g) ($p < 0.05$).

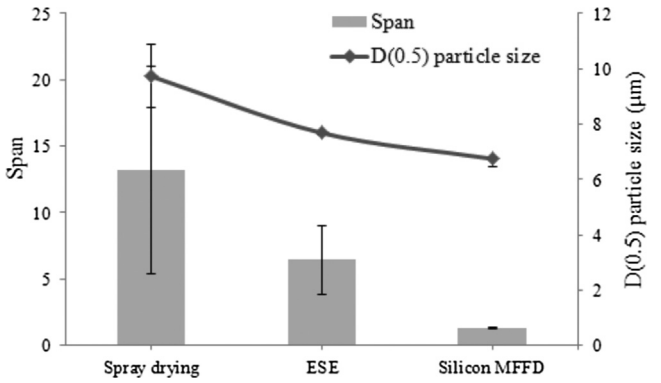

Fig. 4. Microparticle size and span distribution obtained with silicon MFFD devices and compared against conventional production techniques. All experiments were conducted using PLGA (low viscosity) polymer. Data represents the mean SD ($n = 3$).

Drug release from PEG-PLGA microparticles was significantly faster than PLGA ($p < 0.05$) (Fig. 8). After 24 h, 96 ± 4.29% and 92 ± 2.21% of CsA was released from the polymer using MFFD and ESE techniques, respectively. No significant difference in %CsA released was observed between the two methods. By comparison, the rate of release after 24 h from PLGA microparticles using the spray drying, ESE and MFFD techniques was negligible (0.56 ± 0.33%, 0%, 0%, respectively). Hence, the incorporation of a hydrophilic PEG side chain within the microparticle resulted in faster CsA release.

4. Discussion

The control of size and surface characteristics on the biodistribution and release of drug loaded microparticles is important to achieving an optimal pharmacokinetic effect (Kost and Langer, 2001). Therefore, there is a need to develop novel 'bottom-up' microfabrication techniques for the precise control of size and shape of drug loaded microparticles. Microfluidic technologies are emerging as innovative tools for controlling fluid dynamics in microchannels, therein enabling size-tunable droplet formation (Kang et al., 2008). The findings of the current study demonstrate the potential of silicon MFFDs to advance the current state-of-the-art in 'bottom-up' microparticle production processes and the utility thereof in overcoming limitations of conventional 'top-down' approaches for the production of monodisperse PLGA based microparticles.

Table 2
Composition of the microparticles prepared using MFFD and conventional production techniques.

Process conditions	ESE	Spray drying	MFFD
PLGA conc. (% w/v)	4	4	4
CsA loading (%)	16.7	16.7	16.7
Solvent Phase	DCM	DCM	DCM
Aqueous phase (% w/v)	1% PVA	–	1% PVA

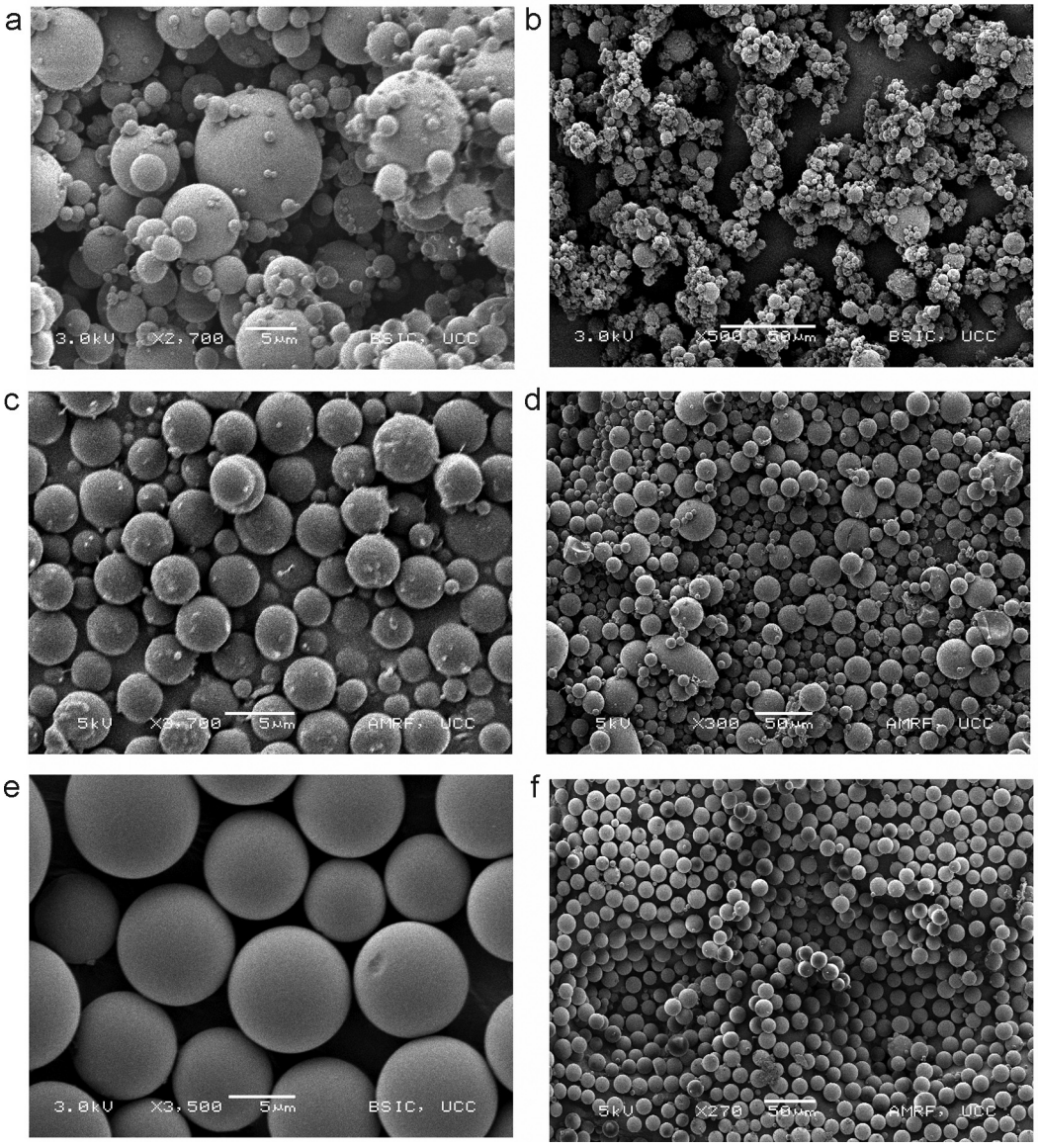

Fig. 5. Representative scanning electron microscopic images of PLGA (low viscosity) microparticles produced from various processing techniques. (A) and (B) spray drying, (C) and (D) ESE (E) and (F) silicon MFFD.

The ability to produce monodisperse microparticles using MFFDs is dependent, however, on a number of key experimental parameters that govern uniform droplet break up at the flow focusing channel. Critical experimental parameters identified were the flow rates, the ratio of Q_d:Q_c, polymer type and polymer concentration. A clear relationship between fluid dynamics in the microchannels and microparticle size was demonstrated, with a near linear relationship observed between *Ca* number and microparticle size within the size range of 5–24 μm (Fig. 3c). A similar relationship between *Ca* number and droplet size has previously been reported, which reflects the impact of these changes in *Ca* number on droplet break up (Tan et al., 2004).

Table 3
Results of processing conditions on the encapsulation efficiency, particle size and specific surface area of PLGA and PEG-PLGA based microparticles. Data represents the mean SD ($n = 3$).

Process	Encapsulation efficiency		Actual yield		Particle size (μm)		Specific surface (BET)	
	%	±SD	%	±SD	d(0.5)	±SD	m^2/g	±SD
ESE	69	2	73	2	7.6	0.1	1.15	0.01
Spray drying	54	5	46	15	9.7	1.2	2.13	0.02
Silicon MFFD	95**	5	73	3	6.7	0.3	1.57	0.02
–								
ESE[a]	68	1	76	2	14.9	2.0	1.26	0.01
Silicon MFFD[a]	93**	2	76	6	15.4	0.1	7.32*	0.02

* $p < 0.05$ vs ESE.
** $p < 0.01$ vs spray drying and ESE.
[a] Microparticles produced using PEG-PLGA copolymer.

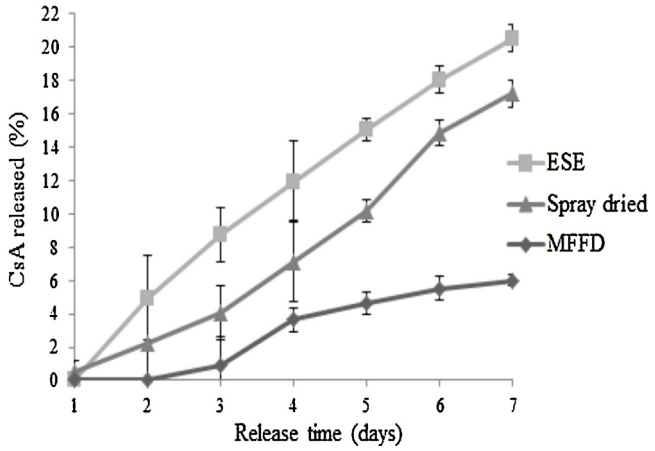

Fig. 6. Comparison of *in-vitro* Ciclosporin A release profiles from PLGA microparticles prepared using silicon MFFDs and conventional ESE and spray drying techniques. Data represents the mean ± SD ($n = 3$).

However, while a linear relationship between droplet size and *Ca* number was evident at the flow rates used in the current study, it cannot be inferred that at higher flow rates (i.e. increasing *Ca*) further decreases in droplet sizes may be predicted. On the contrary, Stan et al. (2009) demonstrated that over an extended range of *Ca* numbers, the relationship between *Ca* and droplet size was best predicted using a logarithmic model and that at higher *Ca* numbers, droplet sizes appeared to plateau (Stan et al., 2009).

MFFDs offer a number of potential advantages in the production of biodegradable microparticles, compared to conventional technologies. The MFFD approach offered precise control of microparticle size, with a monodisperse size distribution (i.e. less polydispersity), compared to ESE and spray drying (Fig. 4). The reduced shear stresses using MFFDs compared to ESE may assist in maintaining the bioactivity of shear sensitive biopharmaceutical drugs, such as proteins (Xu et al., 2009). In addition, MFFDs produced microparticles at ambient temperatures, unlike spray drying, which utilises elevated temperatures to evaporate aqueous and organic solvents. Furthermore, a change in microparticle size was readily obtained by altering flow rates (i.e. *Capillary* number). Conventional methods of manufacturing can lead to polydisperse batch sizes, due to the random nature of microparticle formation (Vladisavljević et al., 2014). While a number of studies have evaluated the impact of processing conditions on microparticle size using both ESE and spray drying, the relationships obtained were complex, involving a number of processing parameters (Rizi et al., 2011; Nilkumhang and Basit, 2009).

Higher drug loading efficiencies were observed utilising the MFFD approach (95 ± 5%), relative to both ESE and spray drying, most likely reflecting a greater extent of drug loss using the conventional process techniques. In addition, processing via MFFDs was found to influence drug release characteristics, with a slower CsA release from PLGA microparticles compared to similar size microparticles produced using the conventional "top-down" techniques. The delayed release of CsA through the PLGA matrix most likely reflects the rate limiting diffusional mass transport through the polymer core. It is hypothesised that with the spray drying and ESE processes, the continuous breakup of larger droplets into smaller droplets may lead to more surface bound drug and less homogenous drug distribution within the microparticle core. Consequently, drug release may be faster using these approaches. However, the "bottom-up" approach using MFFDs may result in less drug migration to the surface of the microparticles, more homogeneous distribution within the polymeric core and slower drug release from the microparticles. This hypothesis may also be used to support the observation of a higher encapsulation efficiency obtained during processing via MFFDs reflecting lower drug loss from the surface of the microparticles into the external aqueous phase.

A comparison of PEG-PLGA microparticles produced using MFFDs and ESE confirmed the potential of the MFFD approach to

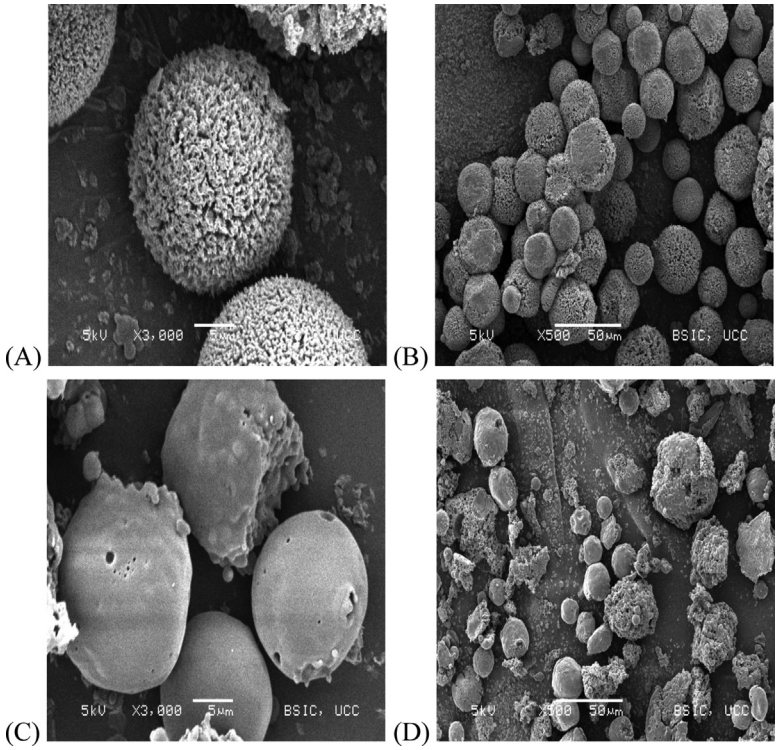

Fig. 7. Scanning electron microscopy images of; (A) and (B) MFFD produced porous PEG-PLGA microparticles and (C) and (D) ESE produced PEG-PLGA microparticles.

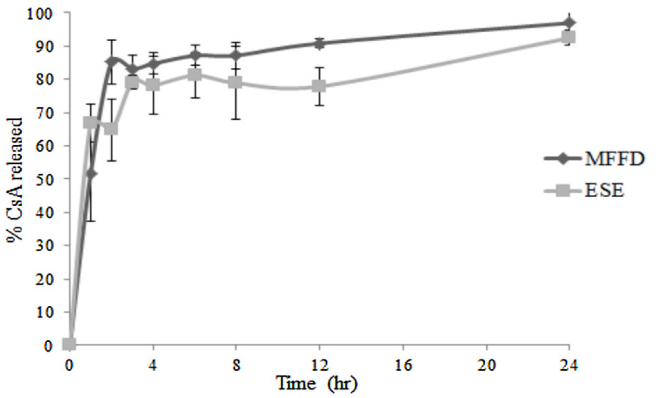

Fig. 8. Comparison of *in-vitro* Ciclosporin A release profiles from PEG-PLGA microparticles prepared using silicon MFFDs and conventional ESE. Data represents the mean ± SD ($n = 3$).

influence the surface morphology of PLGA microparticles. The benefits of incorporating a PEG moiety onto the PLGA structure provides "stealth" properties for immune evasion, which may therefore improve site specific delivery (Avgoustakis, 2004; Karnik et al., 2008). PEG–PLGA has previously demonstrated enhanced translocation and deposition in inflamed intestinal mucosa compared to non-functionalised PLGA microparticles with potential therapeutic applications in inflammatory bowel disease (IBD) (Lautenschläger et al., 2013). Highly porous and uniform PEG-PLGA microparticles were produced using the MFFD approach (Fig. 7a and b), displaying a larger surface area than non-pegylated microparticles ($7.32 \pm 0.02\ m^2/g$, $1.57 \pm 0.02\ m^2/g$, respectively). Porous microparticles have previously demonstrated potential applications in pulmonary drug delivery, given that the lung has a large surface area (~100–140 m^2) and a highly permeable epithelium for absorption of microparticles >5 μm (Giovagnoli et al., 2007).

The mechanism of drug release from PLGA based microparticles has been previously attributed to a diffusion controlled process from the polymer matrix, followed by hydrolytic degradation of the polymer (Ronneberger et al., 1996; Korber, 2010). In the case of PEG-PLGA, the hydrophilic PEG moiety has been cited as one of the reasons for rapid release of CsA (Patel et al., 2012). Formulations prepared using PEG undergoes initial hydration to form an intermediate diffusion layer. This leads to enhanced wetting of the microparticle, allowing water to penetrate the surface. This subsequently results in the rapid disintegration of the polymer matrix, eroding the polymer and facilitating enhanced drug release (Patel et al., 2012). This was characterised by an initial burst release, where approximately 85% of CsA was released within the first 2 h (Fig. 8). A recent study demonstrated that erosion in the presence of PEG is faster than formulations without PEG and can be controlled by either increasing or decreasing the PEG content (Buske et al., 2012).

Although PDMS is the most commonly used material to fabricate microfluidic chips due to its relative cost effectiveness and ease of fabrication, it displays poor resistance to organic solvents. A surface pre-treatment step (plasma oxidation) has previously shown to increase the longevity of PDMS devices to approximately 5 h (Xu et al., 2009). However, this is dependent on the surface of the microchannels remaining hydrophilic, which can gradually become hydrophobic upon exposure to organic solvents. Another disadvantage of PDMS is its elasticity, which can limit the incorporation of design features with specific aspect ratios due to shrinking or sagging of the MFFD device (Sia and Whitesides, 2003). Alternative microfluidic platforms have been explored, including co-axial glass capillary microfluidic devices, which have recently been reported for the production of monodisperse PLGA-based microspheres (Wu et al., 2013). Although optically transparent, the fabrication of co-axial glass capillaries can be a labour intensive, manual microfabrication process, which is not ideal for large scale-up applications (Vladisavljević et al., 2013). Results from the current study demonstrate the suitability of silicon based MFFDs to withstand the effects of organic solvents, which facilitated extended use and re-use of the chips. This is an important consideration, where continuous long-term operation is critical for industrial scale-up applications of microfluidics technology (Vladisavljević et al., 2013).

5. Conclusions

In this study, CsA loaded PLGA and PEG-PLGA microparticles were successfully prepared using silicon MFFDs. The findings from this study demonstrate the utility of MFFDs for the precise control of size and surface morphology of PLGA based microparticles over an extended period of time. In these experiments, it was possible to control the formation and size of the microdroplets at the flow focusing channel. The results demonstrated that by modifying the polymer type and Q_d:Q_c flow rates, microparticle size could be successfully controlled using silicon MFFDs. A comparison against conventional production techniques resulted in more uniform microparticle sizes, with improved encapsulation efficiency and slower drug release rates. Finally, novel PEG-PLGA microparticles were produced using MFFDs, with a higher surface area, highly porous morphology and faster drug release profile, relative to PLGA microparticles that do not contain a hydrophilic PEG side chain. The findings from this study demonstrate the efficacy of this "bottom-up" microfabrication approach for the production of size-tunable drug loaded PLGA-based microparticles and the utility thereof in overcoming limitations of conventional "top-down" approaches.

Declaration of interest

The authors report no declarations of interest.

Acknowledgements

This work was kindly supported by Science Foundation Ireland strategic research cluster, Irish Drug Delivery Network (Grant no. 07/SRC/B1154). Paul Galvin would like to acknowledge the financial support of Science Foundation Ireland (SFI) under grant numbers SFI/12/RC/2289, SFI 12/RC/2272, SFI 10/CE/B1821 and SFI 07/CE/I1147. The authors would also like to acknowledge the National Access Program (NAP192) and Tyndall National Institute.

Appendix A. Supplementary data

Supplementary data associated with this article can be found, in the online version, at http://dx.doi.org/10.1016/j.ijpharm.2014.03.051.

References

Avgoustakis, K., 2004. Pegylated poly (lactide) and poly (lactide-co-glycolide) nanoparticles: preparation, properties and possible applications in drug delivery. Current Drug Delivery 1, 321–333.
Bashir, R., 2004. BioMEMS: state-of-the-art in detection, opportunities and prospects. Advanced Drug Delivery Reviews 56, 1565–1586.
Bhardwaj, U., Burgess, D.J., 2010. A novel USP apparatus 4 based release testing method for dispersed systems. International Journal of Pharmaceutics 388, 287–294.

Brunauer, S., Emmett, P.H., Teller, E., 1938. Adsorption of gases in multimolecular layers. Journal of the American Chemical Society 60, 309–319.
Buske, J., Konig, C., Bassarab, S., Lamprecht, A., Muhlau, S., Wagner, K., 2012. Influence of PEG in PEG-PLGA microspheres on particle properties and protein release. European Journal of Pharmaceutics and Biopharmaceutics 81, 57–63.
Coimbra, P.A., De Sousa, H.C., Gil, M.H., 2008. Preparation and characterization of flurbiprofen-loaded poly(3-hydroxybutyrate-co-3-hydroxyvalerate) microspheres. Journal of Microencapsulation 25, 170–178.
De Geest, B.G., Urbanski, J.P., Thorsen, T., Demeester, J., De Smedt, S.C., 2005. Synthesis of monodisperse biodegradable microgels in microfluidic devices. Langmuir 21, 10275–10279.
Fu, T., Wu, Y., Ma, Y., Li, H.Z., 2012. Droplet formation and breakup dynamics in micro fluidic flow-focusing devices: from dripping to jetting. Chemical Engineering Science 84, 207–217.
Gañán-Calvo, A., Montanero, J., Martín-Banderas, L., Flores-Mosquera, M., 2013. Building functional materials for health care and pharmacy from microfluidic principles and flow focusing. Advanced Drug Delivery Reviews 65, 1447–1469.
Giovagnoli, S., Blasi, P., Schoubben, A., Rossi, C., Ricci, M., 2007. Preparation of large porous biodegradable microspheres by using a simple double-emulsion method for capreomycin sulfate pulmonary delivery. International Journal of Pharmaceutics 333, 103–111.
Hung, L., Lee, A., 2007. Microfluidic devices for the synthesis of nanoparticles and biomaterials. Journal of Medical and Biological Engineering 27.
Kang, L., Chung, B.G., Langer, R., Khademhosseini, A., 2008. Microfluidics for drug discovery and development: from target selection to product lifecycle management. Drug Discovery Today 13, 1–13.
Karnik, R., Gu, F., Basto, P., Cannizzaro, C., Dean, L., Kyei-Manu, W., Langer, R., Farokhzad, O.C., 2008. Microfluidic platform for controlled synthesis of polymeric nanoparticles. Nano Letters 8, 2906–2912.
Khan, I.U., Serra, C.A., Anton, N., Vandamme, T., 2013. Continuous-flow encapsulation of ketoprofen in copolymer microbeads via co-axial microfluidic device: influence of operating and material parameters on drug carrier properties. International Journal of Pharmaceutics 441, 809–817.
Korber, M., 2010. PLGA erosion: solubility-or diffusion-controlled? Pharmaceutical Research 27, 2414–2420.
Kost, J., Langer, R., 2001. Responsive polymeric delivery systems. Advanced Drug Delivery Reviews 46, 125–148.
Lautenschläger, C., Schmidt, C., Lehr, C.-M., Fischer, D., Stallmach, A., 2013. PEG-functionalized microparticles selectively target inflamed mucosa in inflammatory bowel disease. European Journal of Pharmaceutics and Biopharmaceutics 85, 578–586.
Lo, C.T., Jahn, A., Locascio, L.E., Vreeland, W.N., 2010. Controlled self-assembly of monodisperse niosomes by microfluidic hydrodynamic focusing. Langmuir 26, 8559–8566.
Maa, Y.F., Hsu, C.C., 1999. Performance of Sonication and Microfluidization for liquid–liquid emulsification. Pharmaceutical Development and Technology 4, 233–240.
Mao, S., Shi, Y., Li, L., Xu, J., Schaper, A., Kissel, T., 2008. Effects of process and formulation parameters on characteristics and internal morphology of poly(D,L-lactide-co-glycolide) microspheres formed by the solvent evaporation method. European Journal of Pharmaceutics and Biopharmaceutics 68, 214–223.
Mao, S., Xu, J., Cai, C., Germershaus, O., Schaper, A., Kissel, T., 2007. Effect of WOW process parameters on morphology and burst release of FITC-dextran loaded PLGA microspheres. International Journal of Pharmaceutics 334, 137–148.
Nilkumhang, S., Basit, A.W., 2009. The robustness and flexibility of an emulsion solvent evaporation method to prepare pH-responsive microparticles. International Journal of Pharmaceutics 377, 135–141.
Patel, B., Gupta, V., Ahsan, F., 2012. PEG-PLGA based large porous particles for pulmonary delivery of a highly soluble drug, low molecular weight heparin. Journal of Controlled Release 162, 310–320.
Paudel, A., Worku, Z.A., Meeus, J., Guns, S., Van Den Mooter, G., 2013. Manufacturing of solid dispersions of poorly water soluble drugs by spray drying: considerations. International Journal of Pharmaceutics 453, 253–284.
Petros, R.A., Desimone, J.M., 2010. Strategies in the design of nanoparticles for therapeutic applications. Nature Reviews. Drug Discovery 9, 615–627.
Ramtoola, Z., Lyons, P., Keohane, K., Kerrigan, S.W., Kirby, B.P., Kelly, J.G., 2011. Investigation of the interaction of biodegradable micro- and nanoparticulate drug delivery systems with platelets. Journal of Pharmacy and Pharmacology 63, 26–32.
Ribeiro-Costa, R., Cunha, M.R.R.D., Gongora-Rubio, M., Michaluart-Junior, P., Re, M., 2009. Preparation of protein-loaded-PLGA microspheres by an emulsion/solvent evaporation process employing LTCC micromixers. Powder Technology 190, 107–111.
Rizi, K., Green, R.J., Donaldson, M., Williams, A.C., 2011. Production of pH-responsive microparticles by spray drying: investigation of experimental parameter effects on morphological and release properties. Journal of Pharmaceutical Sciences 100, 566–579.
Ronneberger, B., Kao, W.J., Anderson, J.M., Kissel, T., 1996. In vivo biocompatibility study of ABA triblock copolymers consisting of poly(L-lactic-co-glycolic acid) A blocks attached to central poly(oxyethylene) B blocks. Journal of Biomedical Materials Research 30, 31–40.
Rosca, I.D., Watari, F., Uo, M., 2004. Microparticle formation and its mechanism in single and double emulsion solvent evaporation. Journal of Controlled Release 99, 271–280.
Ruan, G., Feng, S.-S., 2003. Preparation and characterization of poly(lactic acid)-poly(ethylene glycol)-poly(lactic acid) (PLA-PEG-PLA) microspheres for controlled release of paclitaxel. Biomaterials 24, 5037–5044.
Sansdrap, P., Moës, A.J., 1993. Influence of manufacturing parameters on the size characteristics and the release profiles of nifedipine from poly(DL-lactide-co-glycolide) microspheres. International Journal of Pharmaceutics 98, 157–164.
Sia, S.K., Whitesides, G.M., 2003. Microfluidic devices fabricated in poly(dimethylsiloxane) for biological studies. Electrophoresis 24, 3563–3576.
Stan, C.A., Tang, S.K.Y., Whitesides, G.M., 2009. Independent control of drop size and velocity in microfluidic flow-focusing generators using variable temperature and flow rate. Analytical Chemistry 81, 2399–2402.
Tan, Y.-C., Fisher, J.S., Lee, A.I., Cristini, V., Lee, A.P., 2004. Design of microfluidic channel geometries for the control of droplet volume, chemical concentration, and sorting. Lab on a Chip 4, 292–298.
Vladisavljević, G.T., Khalid, N., Neves, M.A., Kuroiwa, T., Nakajima, M., Uemura, K., Ichikawa, S., Kobayashi, I., 2013. Industrial lab-on-a-chip: design, applications and scale-up for drug discovery and delivery. Advanced Drug Delivery Reviews 65, 1626–1663.
Vladisavljević, G.T., Shahmohamadi, H., Das, D.B., Ekanem, E.E., Tauanov, Z., Sharma, L., 2014. Glass capillary microfluidics for production of monodispersed poly(DL-lactic acid) and polycaprolactone microparticles: experiments and numerical simulations. Journal of Colloid and Interface Science 418, 163–170.
Whitesides, G.M., 2006. The origins and the future of microfluidics. Nature 442, 368–373.
Wu, J., Kong, T., Yeung, K.W.K., Shum, H.C., Cheung, K.M.C., Wang, L., To, M.K.T., 2013. Fabrication and characterization of monodisperse PLGA-alginate core–shell microspheres with monodisperse size and homogeneous shells for controlled drug release. Acta Biomaterialia 7410–7419.
Xu, Q., Hashimoto, M., Dang, T.T., Hoare, T., Kohane, D.S., Whitesides, G.M., Langer, R., Anderson, D.G., 2009. Preparation of monodisperse biodegradable polymer microparticles using a microfluidic flow-focusing device for controlled drug delivery. Small 5, 1575–1581.
Yager, P., Edwards, T., Fu, E., Helton, K., Nelson, K., Tam, M.R., Weigl, B.H., 2006. Microfluidic diagnostic technologies for global public health. Nature 442, 412–418.
Yeh, C.-H., Zhao, Q., Lee, S.-J., Lin, Y.-C., 2009. Using a T-junction microfluidic chip for monodisperse calcium alginate microparticles and encapsulation of nanoparticles. Sensors and Actuators A: Physical 151, 231–236.
Zhang, Y., Chan, H.F., Leong, K.W., 2013. Advanced materials and processing for drug delivery: the past and the future. Advanced Drug Delivery Reviews 65, 104–120.